

# Self-organized distribution of periodicity and chaos in an electrochemical oscillator

Melke A. Nascimento,<sup>a</sup> Jason A. C. Gallas<sup>bc</sup> and Hamilton Varela<sup>\*a</sup>

Received 30th June 2010, Accepted 7th September 2010

DOI: 10.1039/c0cp01038c

We report a detailed numerical investigation of a prototype electrochemical oscillator, in terms of high-resolution phase diagrams for an experimentally relevant section of the control (parameter) space. The prototype model consists of a set of three autonomous ordinary differential equations which captures the general features of electrochemical oscillators characterized by a partially hidden negative differential resistance in an N-shaped current–voltage stationary curve. By computing Lyapunov exponents, we provide a detailed discrimination between chaotic and periodic phases of the electrochemical oscillator. Such phases reveal the existence of an intricate structure of domains of periodicity self-organized into a chaotic background. Shrimp-like periodic regions previously observed in other discrete and continuous systems were also observed here, which corroborate the universal nature of the occurrence of such structures. In addition, we have also found a structured period distribution within the order region. Finally we discuss the possible experimental realization of comparable phase diagrams.

## Introduction

Among chemically reacting systems, electrochemical ones probably comprise the most paradigmatic class, with examples ranging from electrodisolution of metals to electrocatalytic oxidation of small organic molecules.<sup>1–3</sup> Complex response in electrochemical systems results from the interplay among the kinetics itself, transport processes (reactants to, and products from the electrode surface) and electrical circuit. In particular for the case of fuel cell relevant reactions, such as the catalytic electro-oxidation of hydrogen and small organic molecules, oscillatory kinetics has been extensively observed.<sup>4–6</sup> From the experimental perspective, multi-stability, periodic and mixed-mode oscillations, and chaos have been observed in the temporal domain,<sup>7–10</sup> whereas many different spatiotemporal patterned states including travelling pulses, target patterns, clusters and turbulence<sup>11–14</sup> have been reported. Those findings unquestionably put such systems in a privileged position among electrochemical systems. From the theoretical point-of-view, the vast majority of numerical studies in those systems are based in continuation methods and mostly focused on the investigation of conventional bifurcation diagrams delimitating regions of occurrence of steady states, bistability, oscillations, *etc.* In terms of the dynamic behavior within the oscillatory region, numerical studies consist of the calculation of few time-series, and thus cover relatively small parameter regions. Although very useful and illustrative, this approach is somewhat limited in the sense that it often neglects the fine structure within the oscillatory region and thus might oversee interesting

behavior. Two-dimensional phase diagrams can provide a comprehensive and detailed description of the system, since they display dynamical features in relevant two-parameter sections, and discriminate simultaneously order regions, with different types of periodic motions, and regions with chaotic phases. Phase diagrams also reveal the nature of the boundaries, smooth or fractal, between distinct oscillatory modes.

Two-dimension high-resolution phase diagrams are rather common for discrete-time models described by maps.<sup>15–18</sup> In contrast, because of the high computational cost involved, this approach has been far less applied for continuous-time autonomous models consisting of sets of nonlinear differential equations. For a survey, see ref. 19. The few examples available of phase diagrams in continuous-time models include applications in CO<sub>2</sub> lasers, *etc.*<sup>20–22</sup> As far as chemical reactions are concerned, there is apparently only one example: the Belousov–Zhabotinsky reaction.<sup>23</sup> The authors used the model proposed by Gyorgyi and Field<sup>24</sup> which consists of three nonlinear differential equations and 14 parameters.

We report in this work a detailed numerical investigation of a minimal model of a generic electrochemical oscillator. Specifically, we compute high-resolution phase diagrams for an experimental relevant section of the control (parameter) space of a prototype electrochemical oscillator<sup>25,26</sup> and further explore the structure within a periodic domain embedded in a chaotic background. In contrast to other traditional methodologies, the approach adopted here is unique in the sense that it describes in depth the boundaries of chaotic phases and also the inner structure of those phases.

## Model and numerical procedures

The electrochemical model investigated here is a generic one proposed by Krischer,<sup>3</sup> who merged and improved the earlier work by Koper<sup>25,26</sup> for two types of electrochemical oscillators. The resulting model is an interesting prototype to be used in

<sup>a</sup> Instituto de Química de São Carlos, Universidade de São Paulo, CP-780, CEP: 13560-970, São Carlos-SP, Brazil.

E-mail: varela@iqsc.usp.br

<sup>b</sup> Departamento de Física, Universidade Federal da Paraíba, CEP: 58051-970, João Pessoa-PB, Brazil

<sup>c</sup> Instituto de Física, Universidade Federal do Rio Grande do Sul, CEP: 91501-970, Porto Alegre-RS, Brazil

the study of mixed mode oscillations and other complex phenomena observed in a certain class of electrochemical systems, which includes most of the fuel cell anodic reactions.<sup>3,5</sup> The model consists of three ordinary differential equations (ODEs) accounting for the temporal evolution of the double layer potential ( $\phi$ ), the concentration of electroactive species ( $c$ ) and the surface coverage of an inhibiting species ( $\theta$ ). The time evolution of double layer potential reads,

$$\varepsilon \frac{d\phi}{dt} = -ck(\phi)(1 - \theta) + \frac{U - \phi}{\rho} \quad (1)$$

where  $\varepsilon$  is the time-scale for the evolution of the electrode potential,  $c$  is the concentration of the electroactive species,  $k(\phi)$  is the potential-dependent reaction rate constant,  $\theta$  is the surface coverage of a poison species that blocks the faradaic reaction,  $U$  is the applied voltage, and  $\rho$  is the total resistance. The left-hand-side term in eqn (1) is the capacitive current, whereas the rhs terms are the faradaic and the total current, respectively.

The surface coverage of poisoning species,  $\theta$ , obeys<sup>3</sup>

$$\frac{d\theta}{dt} = \theta_0(\phi) - \theta, \quad (2)$$

where the stationary poison coverage is described by a suitable function  $\theta_0(\phi)$  (see eqn (4) below). Finally, the concentration of active species at the reaction plane,

$$\mu \frac{dc}{dt} = -ck(\phi)(1 - \theta) + 1 - c. \quad (3)$$

The term  $\mu$  accounts for the time-scale of the temporal evolution of  $c$ . Eqn (1)–(3) represent the dimensionless version of the model, details on their derivation can be found in ref. 3, 25 and 26.

The stationary dependence of the poison coverage on the electrode potential,  $\theta_0(\phi)$ , follows the equation suggested by Koper and Sluyters<sup>27</sup> and reads,

$$\theta_0(\phi) = \left[ 1 + \exp\left(\frac{\phi - \phi_0}{b}\right) \right]^{-1}. \quad (4)$$

Simulations were carried out with  $b = 7.12$  and  $\phi_0 = 124.6$ . The rate constant,  $k(\phi)$ , is described by the polynomial equation,

$$k(\phi) = 0.00002\phi^3 - 0.0094\phi^2 + 1.12\phi, \quad (5)$$

which essentially represents the negative differential resistance (NDR) in a N-shaped current–potential curve.

The system under consideration display oscillations under both galvanostatic (constant current) and potentiostatic (constant potential) control modes. Under potentiostatic control, oscillations are only found for a finite resistance between the working electrode and the potentiostat (either the ohmic drop through the electrolyte or a resistor deliberately inserted, or, more generally, the sum of both contributions). Different oscillatory patterns are found according to the pair total resistance  $\times$  applied voltages, so that, the dynamics of these systems under potentiostatic regime is routinely mapped in this plane, as in the present case.

Eqn (1)–(3) were numerically integrated using Matlab. Conventional bifurcation diagrams were obtained with Matcont continuation toolbox.<sup>28</sup> The determination of Lyapunov

exponents was based on the algorithm suggested by Wolf *et al.*<sup>29</sup> Phase diagrams have resolutions of  $500 \times 500$  exponents (Fig. 2) or  $700 \times 700$  (Fig. 3(a) and (b)) exponents, and were calculated with steps of 0.01 for the Lyapunov diagrams and of 0.001 for the period diagram.

Parameter grid points were color codified according to the magnitude of the largest nonzero Lyapunov exponent. Regions of negative exponent (periodic solution) are generically referred to as periodic regions, in opposition to chaotic ones. The positive values (chaotic oscillation) are indicated in a yellow-red scale.

## Results and discussion

Fig. 1(a) shows the main features of the model in terms of the N-shaped curve (black), the adsorption isotherm of poisoning species (red), and the overall faradaic curve (blue). As apparent in this figure, the negative differential resistance in the N-shaped original (black) curve is partially hidden by the adsorption of the poisoning species, which blocks the electrode surface inhibiting thus the oxidation of the electroactive species. The resulting (blue) curve is fully comparable to that observed in many experimental systems.<sup>9,10</sup> As in the case of experimental examples in this class, the generic model of the HN-NDR electrochemical oscillator<sup>2,3</sup> discussed here supports current oscillations for some combination of  $U$  and  $\rho$ , as well as potential oscillations under galvanostatic regime (not discussed here). Fig. 1(b) and (c) illustrate the oscillatory response of the faradaic current, *i.e.* the overall reaction rate, for a given overall resistance and two different applied voltages. Fig. 1(b) shows a periodic response whereas in (c) a chaotic time series obtained at slightly higher  $U$  is exemplified. The evolution of this chaotic state is illustrated in Fig. 1d in terms of three-dimension phase space with  $\phi$ ,  $c$ , and  $\theta$ .

The system of eqn (1)–(3) was extensively investigated by conventional methods and bifurcation analysis, and found to oscillate in a considerably wide parameter range. In order to allow the comparison with experimental data, parameters  $U$  and  $\rho$  are the most straightforward to be investigated under potentiostatic regime. Therefore, we calculate high-resolution phase diagrams in the  $U$  versus  $\rho$  plane for a given set of parameters. Fig. 2 shows examples of high-resolution phase diagrams for  $\varepsilon = 0.001$  and  $\mu = 50$ . In all cases, negative and zero Lyapunov exponents, *i.e.* regions characterized by periodic solutions, are given in black while positive exponents are color-codified according to the magnitude of the largest nonzero exponent. The color red indicates regions of “stronger” chaos, namely regions characterized by positive Lyapunov exponents of larger magnitude. Regions highlighted by white rectangles are shown magnified in the subsequent plate. The highlighted region in Fig. 2(d) is shown magnified in Fig. 3. The shape of the black/yellow oscillatory region in Fig. 2(a) is very similar to the region confined by the Hopf line in the  $U$  versus  $\rho$  plane for this class of electrochemical oscillator as evidenced in both experiments and modeling.<sup>30–32</sup> The yellow ‘lines’ inside the black background account for the parameter domains where chaotic dynamics is observed, *i.e.* regions of positive Lyapunov exponents. Rather than simply chaotic lines, however, intricate patterns emerge when zooming

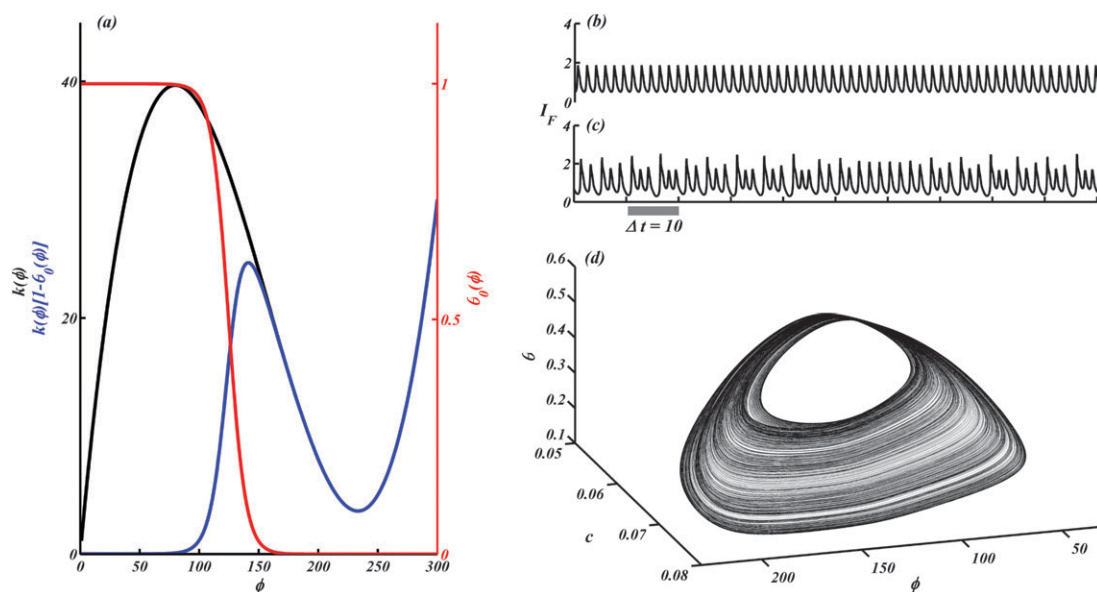


**Fig. 1** (a) Stationary profiles of the NDR contribution (black line), blocking species (red line) and the faradaic current (blue line) as a function of the electrode potential. (b), (c) Reaction current time series for periodic and chaotic dynamics, obtained for  $\rho = 106.7$ , and  $U = 244$  and  $U = 246$ , respectively. (d) Tridimensional attractor for the time series given in panel (c).  $\varepsilon = 0.001$  and  $\mu = 50$ .

specified regions. As an example, focusing on the region in which those lines seem to converge, it is possible to distinguish a very rich substructure of chaotic domains, *viz.* Fig. 2(b). A concentric series of alternating chaotic and periodic regions is

clearly observed around the inferior right-corner of Fig. 2(b). Both the general distribution presented in panel (a) and the concentric structures resemble the numerical results obtained recently for the BZ reaction.<sup>23</sup> In addition to regions with well

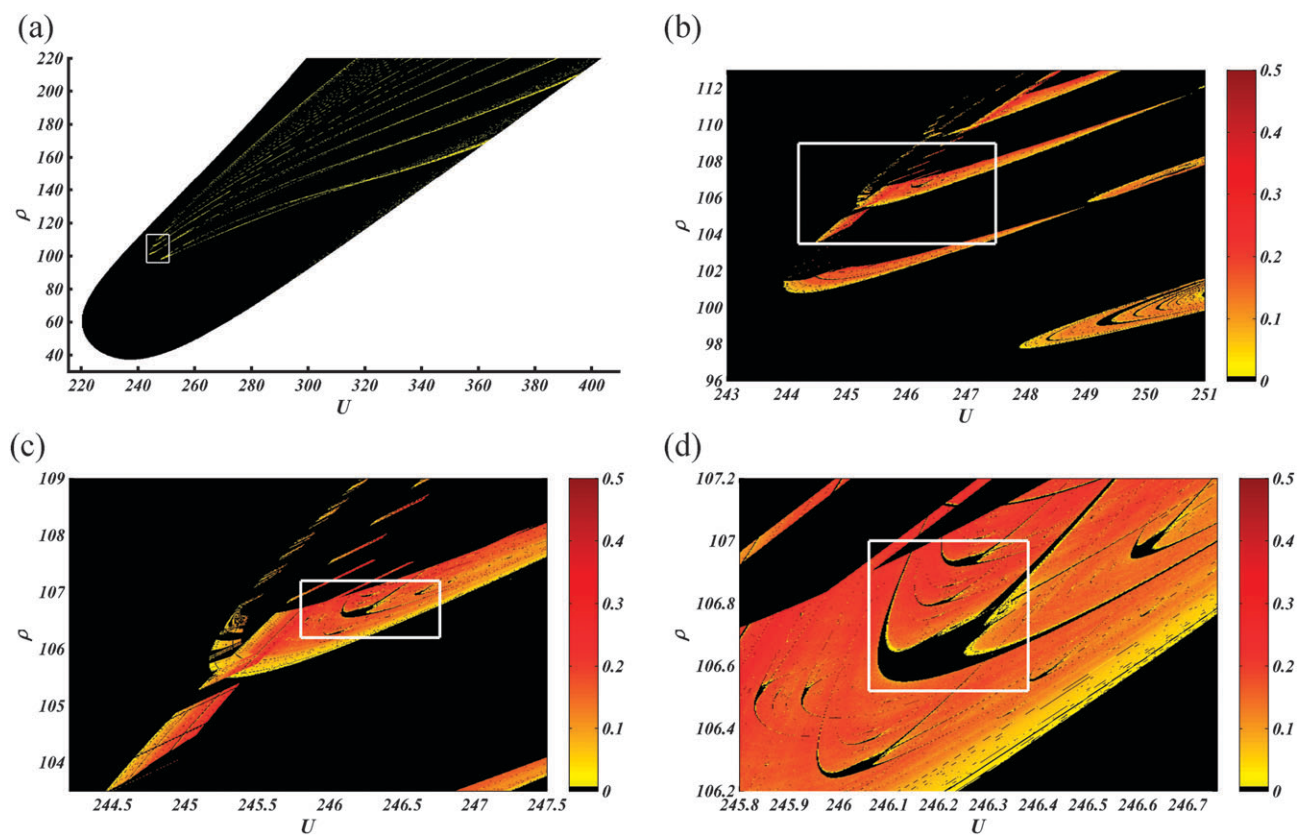


**Fig. 2** High-resolution phase diagrams for the generic HN-NDR model (eqn (1)–(3)) in the  $U$  versus  $\rho$  plane for  $\varepsilon = 0.001$  and  $\mu = 50$ . The color-code accounts for the largest Lyapunov exponent: black denotes order regions with negative or zero exponent, and the yellow to red scale codifies the magnitude of the positive exponents.

defined curved borders, Fig. 2(c) also shows chaotic domains which display abrupt interruptions, *i.e.* not to vary smoothly with the parameters. In fact, such discontinuities are only apparent, indicating the presence of multistability, namely the existence of more than one stable attractor, the one shown depending on the initial conditions. It would be interesting to compute basins of attraction in these parameter domains, to quantify which chemical oscillation dominates as well as the structure of the basins, if fractal or not. Fig. 2(d) illustrates the presence of a series of shrimp-shaped regions of different sizes embedded in the chaotic background in the so-called window streets.<sup>18</sup> The presence of those objects further reinforces the

universal nature of their occurrence, as previously reported for a wide range of continuous-time models.<sup>19,21</sup> It is important to emphasize that shrimps are connected with several non-standard (*i.e.* nonperiod-doubling) routes to chaos. Hubs and spirals have recently explained period-adding routes, arising from cutting highly symmetric spirals in parameter space. Overall, many other routes exist, some so intricate as to be difficult to be described by words, thus the diagrams showing how they develop as parameters are tuned. Similar structures as well as more intricate ones were observed for different values of  $\varepsilon$  and  $\mu$ , and will be reported in due course.<sup>33</sup>

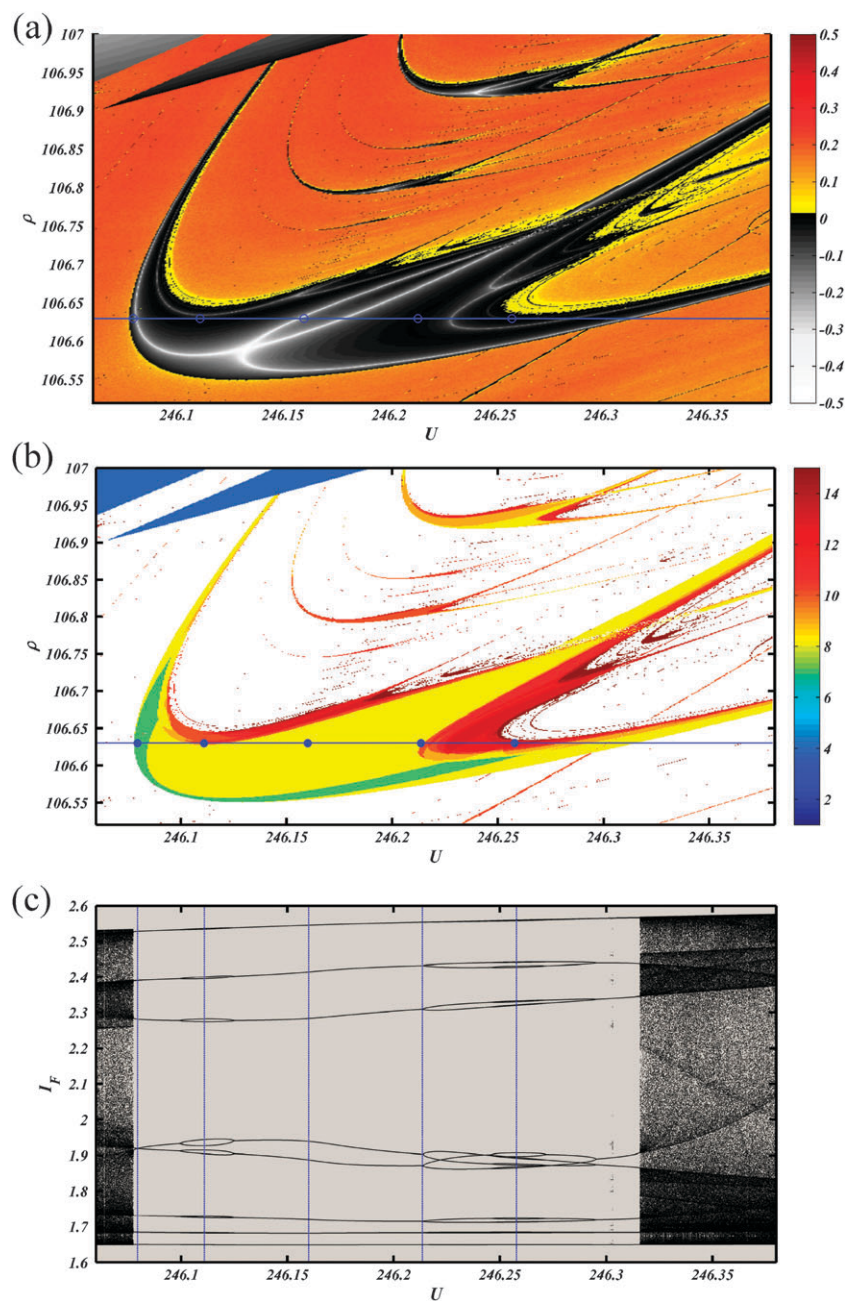


**Fig. 3** (a) High resolution Lyapunov diagram and (b) the corresponding diagram accounting for the oscillation period within the periodic region (see text for details), in the  $U$  versus  $\rho$  plane. (c) Conventional bifurcation diagram for the horizontal cut given in (a) and (b). Remaining conditions as in Fig. 2.

Fig. 3(a) shows a detailed view of the selected region in Fig. 2(d). Differently from that of Fig. 2, however, the magnitude of the negative Lyapunov exponents is also color-coded in the gray scale. As clearly seen, a white line consisting of more negative exponents crosses the shrimp domain in an organized and, apparently, symmetric manner. Fig. 3(b) displays the numerically estimated period distribution in the same parameter region given in (a). Here the chaotic region was deliberately set to zero and coded in white, the periodic states are given in color. Overall, most of the shrimps displayed in this region have periods of about 8, which is considerably higher than the low periods observed in the periodic regions with sharp borders. As illustrated for the main shrimp, those periodic regions are not characterized by a single period, instead, a continuous evolution of the period distribution inside the shrimps is observed. In the example of the main shrimp shown, periods smaller and larger than 8 appear in specific directions, mainly in the border between order and chaotic domains. The periods observed along the horizontal line at  $\rho = 106.63$  in the indicated  $U$  values amount to 7, 12, 8, 8 just prior to the period doubling bifurcation in five branches, leading to a period 13 and 14. This peculiar organization is more evident in the conventional bifurcation diagram given in plate (c), and its comparison with the period diagram in (c) is straightforward. It should be stressed at this point the advantages of working with these high-resolution diagrams: the structuring observed in the  $U$  versus  $\rho$  plane is a genuine two-parameter (codimension-two) phenomenon which is not captured in conventional one-parameter bifurcation diagrams such as the one in Fig. 3(c). High-resolution phase diagrams are unique in the comprehensive description of the fine-structure of generic two-dimensional phenomena.

## Conclusions and outlook

We have described a numerical study of a generic model for an electrochemical oscillator. The analysis was carried out by means of an in-depth investigation of the high-resolution phase diagrams in an experimentally relevant two-parameter plane. This is the first analysis of this kind for an electrochemical system, represented here by a minimal (3 ODEs) continuous-time autonomous model. Computation of Lyapunov exponents provided a detailed discrimination of chaotic and periodic domains and revealed the existence of intricate structuring of periodic domains embedded in a chaotic background. Shrimp-like periodic regions previously observed in other distinct systems were also clearly detected here, which corroborate the universal nature of the appearance of such structures. In addition, we have also found a structured period distribution within the periodic region. Our theoretical prediction shows where to expect specific dynamical behaviors that go beyond what is presently known. Further, our phase diagrams suggest to the experimentalists what sort of precision is required in order to discriminate the complex alternation of periodic and chaotic windows present in the phase diagrams.

In spite of the unambiguous observation of shrimp-like order regions as well as other self-similarities and structuring in different discrete and continuous models, systematic experimental equivalent of the high-resolution phase diagrams such

as the ones reported here are very rare. A recent example of shrimp-like domains was observed in experiments using a version of the Nishio–Inaba circuit.<sup>34</sup> The main difficulty in obtaining such diagrams in chemical or biological systems is connected to the actual size of the parameter region in which such structures are observed in experiments. If such structures occur in relatively small parameter region, as it has been observed in most cases, it turns to be a rather challenging task to discover them experimentally in bi-dimensional phase diagrams. In this respect, we believe that electrochemical systems are realistic candidates to such experimental studies. As already mentioned, most electrochemical systems are known to display oscillatory kinetics under some conditions, this is especially true for the electrochemical oxidation of small organic molecules. Most important, spontaneous long-term surface transformations<sup>8,10,35</sup> can be used as a bifurcation parameter for continuously varying the systems conditions and thus access otherwise hidden states. We are currently working in this direction.

## Acknowledgements

The authors acknowledge Fundação de Amparo à Pesquisa do Estado de São Paulo (FAPESP, MAN # 07/04522-0, HV # 09/07629-6) and Conselho Nacional de Desenvolvimento Científico (CNPq, HV # 302698/2007-8) for financial support. JACG thanks CNPq and AFOSR, grant, FA9550-07-1-0102, for support. He also thanks CESUP-UFRGS for granting computer time.

## References

- 1 J. L. Hudson and T. T. Tsotsis, *Chem. Eng. Sci.*, 1994, **49**, 1493.
- 2 M. T. M. Koper, *Oscillations and complex dynamical bifurcations in electrochemical systems*, in *Advances in Chemical Physics*, ed. I. Prigogine and S. A. Rice, Wiley, New York, 1996, vol. 92, p. 161.
- 3 K. Krischer, *Principles of spatial and temporal pattern formation in electrochemical systems*, in *Modern Aspects of Electrochemistry*, ed. B. E. Conway, J. Bockris and R. White, Kluwer Academic/Plenum Publishers, New York, 1999, vol. 32, p. 1.
- 4 M. Hachkar, B. Beden and C. Lamy, *J. Electroanal. Chem.*, 1990, **287**, 81.
- 5 K. Krischer and H. Varela, *Oscillations and other dynamic instabilities*, in *Handbook of Fuel Cells: Fundamentals Technology, Applications*, ed. W. Vielstich, A. Lamm and H. A. Gasteiger, John Wiley & Sons, Chichester, 2003, vol. 2, p. 679.
- 6 S. Uhm, H. J. Lee and J. Lee, *Phys. Chem. Chem. Phys.*, 2009, **11**, 9326.
- 7 M. Schell, F. N. Albahadily, J. Safar and Y. Xu, *J. Phys. Chem.*, 1989, **93**, 4806.
- 8 H. Okamoto, N. Tanaka and M. Naito, *J. Phys. Chem. A*, 1998, **102**, 7343.
- 9 R. Nagao, I. R. Epstein, E. R. Gonzalez and H. Varela, *J. Phys. Chem. A*, 2008, **112**, 4617.
- 10 E. Boscheto, B. C. Batista, R. B. Lima and H. Varela, *J. Electroanal. Chem.*, 2009, **642**, 17.
- 11 K. Krischer, N. Mazouz and P. Grauel, *Angew. Chem., Int. Ed.*, 2001, **40**, 851.
- 12 J. Lee, J. Christoph, P. Strasser, M. Eiswirth and G. Ertl, *J. Chem. Phys.*, 2001, **115**, 1485.
- 13 H. Varela, C. Beta, A. Bonnefont and K. Krischer, *Phys. Chem. Chem. Phys.*, 2005, **7**, 2429.
- 14 H. Varela, C. Beta, A. Bonnefont and K. Krischer, *Phys. Rev. Lett.*, 2005, **94**, 174104.
- 15 J. A. C. Gallas, *Phys. Rev. Lett.*, 1993, **70**, 2714.
- 16 J. A. C. Gallas, *Physica A (Amsterdam)*, 1994, **202**, 196.

- 
- 17 J. A. C. Gallas, *Appl. Phys. B: Lasers Opt.*, 1995, **60**, S203.
- 18 E. N. Lorenz, *Physica D (Amsterdam)*, 2008, **237**, 1689.
- 19 J. A. C. Gallas, *Int. J. Bifurcation Chaos Appl. Sci. Eng.*, 2010, **20**, 197.
- 20 J. G. Freire, C. Bonatto, C. C. daCamara and J. A. C. Gallas, *Chaos*, 2008, **18**, 033121.
- 21 C. Bonatto and J. A. C. Gallas, *Philos. Trans. R. Soc. London, Ser. A*, 2008, **366**, 505.
- 22 C. Bonatto, J. A. C. Gallas and Y. Ueda, *Phys. Rev. E: Stat., Nonlinear, Soft Matter Phys.*, 2008, **77**, 026217.
- 23 J. G. Freire, R. J. Field and J. A. Gallas, *J. Chem. Phys.*, 2009, **131**, 044105.
- 24 L. Gyorgyi and R. J. Field, *Nature*, 1992, **355**, 808.
- 25 M. T. M. Koper, *Electrochim. Acta*, 1992, **37**, 1771.
- 26 M. T. M. Koper and J. H. Sluyters, *J. Electroanal. Chem.*, 1994, **371**, 149.
- 27 M. T. M. Koper and J. H. Sluyters, *J. Electroanal. Chem.*, 1991, **303**, 73.
- 28 <http://www.matcont.ugent.be/>.
- 29 A. Wolf, J. B. Swift, H. L. Swinney and J. A. Vastano, *Physica D (Amsterdam)*, 1985, **16**, 285.
- 30 M. T. M. Koper, P. Gaspard and J. H. Sluyters, *J. Chem. Phys.*, 1992, **97**, 8250.
- 31 F. Plenge, H. Varela, M. Lübke and K. Krischer, *Z. Phys. Chem.*, 2003, **217**, 365.
- 32 A. L. Martins, B. C. Batista, E. Sitta and H. Varela, *J. Braz. Chem. Soc.*, 2008, **19**, 679.
- 33 M. A. Nascimento, J. A. C. Gallas and H. Varela, 2010, in preparation.
- 34 R. Stoop, P. Benner and Y. Uwate, *Phys. Rev. Lett.*, 2010, **105**, 074102.
- 35 E. Sitta, M. A. Nascimento and H. Varela, *Phys. Chem. Chem. Phys.*, 2010, DOI: 10.1039/c002574g, in press.